

See discussions, stats, and author profiles for this publication at: <https://www.researchgate.net/publication/224767699>

Effect of Thiol Pendant Conjugates on Plasmid DNA Binding, Release, and Stability of Polymeric Delivery Vectors

ARTICLE in BIOMACROMOLECULES · APRIL 2012

Impact Factor: 5.75 · DOI: 10.1021/bm3004786 · Source: PubMed

CITATIONS

15

READS

17

6 AUTHORS, INCLUDING:



Addison S Goodley

University of Maryland, College Park

2 PUBLICATIONS 19 CITATIONS

[SEE PROFILE](#)



Silvia Muro

University of Maryland, College Park

85 PUBLICATIONS 2,417 CITATIONS

[SEE PROFILE](#)



Peter Kofinas

University of Maryland, College Park

95 PUBLICATIONS 1,741 CITATIONS

[SEE PROFILE](#)

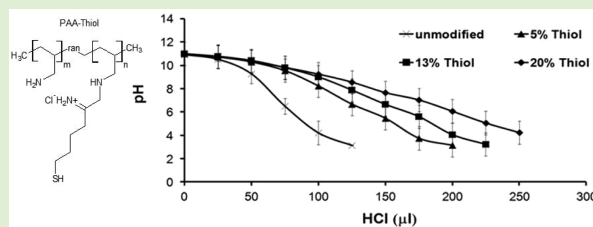
Effect of Thiol Pendant Conjugates on Plasmid DNA Binding, Release, and Stability of Polymeric Delivery Vectors

Irene Bacalocostantis,[†] Viraj P. Mane,[†] Michael S. Kang,[†] Addison S. Goodley,[†] Silvia Muro,^{†,‡} and Peter Kofinas*,[†]

[†]Fischell Department of Bioengineering and [‡]Institute for Bioscience and Biotechnology Research, University of Maryland, College Park, Maryland 20742, United States

Supporting Information

ABSTRACT: Polymers have attracted much attention as potential gene delivery vectors due to their chemical and structural versatility. However, several challenges associated with polymeric carriers, including low transfection efficiencies, insufficient cargo release, and high cytotoxicity levels have prevented clinical implementation. Strong electrostatic interactions between polymeric carriers and DNA cargo can prohibit complete cargo release within the cell. As a result, cargo DNA never reaches the cell's nucleus where gene expression takes place. In addition, highly charged cationic polymers have been correlated with high cytotoxicity levels, making them unsuitable carriers *in vivo*. Using poly(allylamine) (PAA) as a model, we investigated how pH-sensitive disulfide cross-linked polymer networks can improve the delivery potential of cationic polymer carriers. To accomplish this, we conjugated thiol-terminated pendant chains onto the primary amines of PAA using 2-iminothiolane, developing three new polymer vectors with 5, 13, or 20% thiol modification. Unmodified PAA and thiol-conjugated polymers were tested for their ability to bind and release plasmid DNA, their capacity to protect genetic cargo from enzymatic degradation, and their potential for endolysosomal escape. Our results demonstrate that polymer–plasmid complexes (polyplexes) formed by the 13% thiolated polymer demonstrate the greatest delivery potential. At high N/P ratios, all thiolated polymers (but not unmodified counterparts) were able to resist decomplexation in the presence of heparin, a negatively charged polysaccharide used to mimic *in vivo* polyplex–protein interactions. Further, all thiolated polymers exhibited higher buffering capacities than unmodified PAA and, therefore, have a greater potential for endolysosomal escape. However, 5 and 20% thiolated polymers exhibited poor DNA binding-release kinetics, making them unsuitable carriers for gene delivery. The 13% thiolated polymers, on the other hand, displayed high DNA binding efficiency and pH-sensitive release.



INTRODUCTION

Successful gene therapy requires the implementation of safe and efficient carriers that can transverse a number of intracellular and extracellular obstacles, including gene packaging, serums stability, cell targeting, cellular uptake, endolysosomal escape, and cargo release.^{1,2} The ease by which polymers can be chemically and structurally modified to overcome some of these barriers has made polymeric carriers an attractive delivery strategy. The molecular weight, polydispersity, chain composition, and chain density of a polymer can be altered to improve its delivery potential.³ In addition, unlike viral vectors, polymers pose less immunogenicity, carry no risk of integrating into the host chromosome, and can be produced in large quantities at low cost.^{4–6} Despite these advantages, most polymeric carriers fail at one or more of the obstacles mentioned above, leading to inefficient gene delivery and high cytotoxicity.^{1,4,7}

In an attempt to create safe and efficient delivery vectors, researchers have turned their focus to disulfide-containing polymers capable of responding to environmental stimuli.^{5,8,9} Disulfides ($-S-S-$) are formed by thiols ($S-H$) in an oxidation reaction. These linkages are relatively stable within the

oxidizing extracellular environment of the cells, but are readily reduced back into thiols in the reducing intracellular environment of cells.⁹ As a result, thiol-containing polyplexes not only exhibit higher complex stability under extracellular conditions, but also have greater intracellular cargo release and lower cytotoxicity than nonthiolated carriers.^{6,8} Previously, disulfide bonds have been used to link nontoxic low molecular weight (LMW) polymer units to develop biocompatible high molecular weight (HMW) carriers.⁵ Disulfide bonds have also been used to improve carrier stability *in vivo* by linking hydrophilic, nonionic polymers with cationic polymeric carriers.⁵

Amine-rich cationic polymers have been primarily employed as gene delivery vectors because of their ability to form self-assembling complexes with cargo DNA via electrostatic interactions between the polymer's positively charged amines and the DNA's negatively charged phosphates. The relative number of amines to phosphates (N/P ratio) determines the complex charge and affects polyplex size and stability.¹⁰ Studies

Received: January 10, 2012

Published: April 19, 2012

have shown that approximately 90% of the negative charges on the DNA phosphate backbone must be overcome for condensation to occur.¹¹ At a sufficient N/P ratio, polymer–DNA polyplexes form spontaneously upon mixing. The resulting particles have a toroidal or rodlike shape ranging from 30 to several 100 nm in diameter.² Studies have demonstrated that complexes formed by HMW polymers have higher transfection efficiencies and greater steric stabilization than LMW polyplexes, but also impart greater cytotoxicities.^{12–17} Several explanations have been given as to why HMW polymers have greater transfection efficiencies. Van de Watering et al. proposed that the smaller polyplex size formed by HMW polymers is more conducive to internalization.¹⁶ Godbey et al. suggested that HMW polymers are more capable of protecting genetic cargo from nucleases.¹⁴ Finally, Georgiou et al. explained that larger polymers can destabilize the cellular membrane more effectively than smaller polymers, thereby facilitating internalization.¹⁵ It is possible that membrane destabilization not only leads to greater transfection efficiencies, but also cell death. Pafiti et al. suggested that the accumulation of HMW polymers at the cellular membrane leads to localized membrane destabilization and decreased cell viability.¹⁷ The effect of HMW polymeric carriers has been demonstrated in both linear and star polymers.^{14,15,17} To achieve the high transfection efficiency levels of HMW polymers while maintaining the relative safety of LMW polymers, researchers have developed bioreducible polymers, which primarily possess disulfide linkages in their backbone.⁵ Disulfide bonds are relatively stable in the oxidizing extracellular space, allowing bioreducible polymers to maintain polyplex structure and stability.^{5,9} Within the reducing intracellular compartments, the disulfide bonds are reduced back into thiols and the polymer degrades into its LMW biocompatible segments. It is expected that bioreducible polyplexes can achieve the high transfection success of HMW polymers while maintaining the lower cytotoxicity of LMW carriers.¹⁸

Disulfide bonds can also be used to increase polyplex stability by linking cationic polymers with hydrophilic, nonionic polymers such as poly(ethylene)glycol (PEG) and *N*-(2-hydroxypropyl) methacrylamide (HMPA).⁵ Polyplex stability *in vivo* depends on polymer structure and N/P ratio or polyplex charge.¹⁰ When systematically administered, cationic polymers electrostatically interact with negatively charged serum proteins, resulting in polyplex destabilization and rapid clearance by the phagocytic cells of the mononuclear phagocyte system (MPS).^{2,4} It is therefore useful to avoid polymer–protein interactions by masking the polymers cationic charge with nonionic polymers such as PEG and HMPA.⁴ By linking hydrophilic polymer segments onto a cationic polymer via disulfide linkages, it is possible to sterically block polymer–protein interactions and increase polyplex solubility.² Studies have shown pegylated polyplexes to have lower toxicity levels and prolonged circulation times in the bloodstream after intravenous administration in comparison to non-PEGylated complexes.¹⁹

Previous studies have focused on incorporating disulfide linkages either within the polymer backbone or as direct linkages between cationic and nonionic polymers in order to increase biocompatibility and serum stability. However, the potential of disulfide cross-links extending from the polymer chain as a means of improving DNA binding efficiency, complex stability, and gene release has not been explored. We

have developed a series of cationic polymers with varying concentrations of thiol pendant chains in an attempt to understand how thiol cross-links affect polymer–DNA interactions, such as polymer–DNA packaging, cargo release, and polyplex stability. Our results show that thiol-pendant chains improve polyplex stability, polymer binding efficiency, buffering capacity, and cargo release. These data provide a better understanding of the dynamic relationship between thiolated polymers and cargo DNA.

METHODS

Materials. Poly(allylamine) solution (PAA; MW 15000) was purchased from PolySciences Inc. 2-Imino thioliolane (2-IT, Traut's reagent) and 5,5'-dithiobis-(2-nitrobenzoic acid) (DNTB; Ellman's reagent) were purchased from Thermo Scientific. Millipore-Amicon Centrifugal Filter Units (MW cutoff of 5000 Da) were purchased from Millipore. pEGFP-N1 (4700 base pairs) was donated by the Dr. Bentley Research Group at the University of Maryland who acquired the plasmid from CLONTECH Laboratories and cloned it with Top 10 competent cells from Invitrogen. Extractions were carried out by HiSpeed Plasmid Maxi Kit purchased from Qiagen. Ethidium bromide and ethylenediaminetetraacetic acid powder (EDTA) were purchased from Fisher Scientific. Heparin sodium salt, phosphate-buffered saline (PBS), pH 7.4, molecular grade, 4',6-diamidino-2-phenylindole (DAPI), DNase I amplification grade, hydrochloric acid (HCl), and sodium hydroxide (NaOH) were purchased from Sigma. A 1kb DNA Ladder, 10X TAE, and agarose were purchased from New England Biolabs, Promega, and Research Products International Corp, respectively. Folded capillary cells and stoppers were purchased from Malvern.

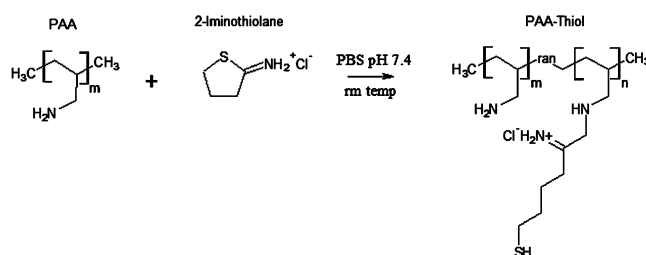


Figure 1. Synthesis of thiolated linear cationic polymer via the substitution of primary amine groups of poly(allylamine) (PAA).

Synthesis of Thiol-PAA. Thiolation of cationic PAA is described in Figure 1. Briefly, PAA was dissolved in 4 mL of PBS, pH 7.4, with 1.75 mg/mL EDTA and reacted with 0.375, 0.75, or 1.5 mg/mL 2-iminothiolane (2-IT) so that 5, 13, or 20% of PAA's primary amines were replaced with thiol-pendant chains (Figure 1). EDTA does not take part in the thiolation reaction but was used to chelate divalent metals in solution, thereby preventing thiol oxidation. The reaction was run at room temperature (RT) for 2 h with continuous shaking on a tabletop orbital shaker. After 2 h, samples were washed twice with PBS using Millipore-Amicon Centrifugal Filter Units. Centrifugation was carried out at 8000g. Washed samples were resuspended in PBS and stored at –80 °C.

Synthesis Verification. Thiolated polymers were characterized by ¹H NMR in D₂O. Degree of thiolation was quantified by a 5,5'-dithiobis-(2-nitrobenzoic acid) (DNTB, Ellman's reagent) assay and verified by ¹H NMR. The DNTB assay was prepared according to manufacturer protocol. Ellman's reagent has been previously used to quantify thiol concentration on thiolated polymers.²⁰ Briefly, 72 µg polymer was suspended in 1 mL of Ellman's buffer with 50 µL of DNTB reagent (2 mg/mL). The absorbance of the polymer solution was measured at 412 nm and the thiol concentration was determined by solving for $c = A \div bE$, where A is the absorbance at 412 nm, b is

the path length in centimeters, E is the molar absorptivity, and c is the concentration in mol/liter (M).

Polyplex Preparation. pEGFP-N1 plasmid (MW 2.9×10^6 Da, 4700 base pairs) was extracted from *E. coli* using the HiSpeed Plasmid Maxi Kit by Qiagen according to kit protocol. pEGFP-N1 is commonly used in delivery studies because it expresses green fluorescent protein (GFP) only upon successful transfection, which is easily detected by UV and fluorescent microscopy.

Polymer–plasmid complexation was carried out by incubating the polymer and plasmid at RT for 45 min at N/P ratios of 1, 5, 10, 20, and 40. The extent of disulfide formation in polyplexes was tested by measuring the concentration of reactive thiols present in solution at initial mixing and after the 45 min incubation period using the previously described DNTB assay.

Determining Binding Efficiency. A DAPI displacement assay was used to determine how thiol cross-links affect the DNA binding efficiency of cationic polymers. Briefly, DAPI was added to pEGFP plasmid and incubated at RT for 30 min to allow the DAPI stain to intercalate into the plasmid strands. For complexation, polymers and DAPI-stained plasmid were mixed and incubated in a 96-well plate at N/P ratios of 1, 5, 10, 20, and 40. Each well consisted of 1 μg plasmid and was brought to a total volume of 100 μL with PBS. Complexation was carried out at RT for 45 min. Fluorescence was read at $\lambda_{\text{ex}} = 360$ nm and $\lambda_{\text{em}} = 455$ nm. Relative fluorescence was determined using the following equation:

$$F_{\text{REL}} = 100 \times (F_{\text{pol}} - F_o) / (F_{\text{DNA}} - F_o)^{21}$$

where F_{pol} is the fluorescence of the polymer–plasmid/DAPI solution, F_{DNA} is the fluorescence of DAPI complexed with plasmid, and F_o is the fluorescence of uncomplexed DAPI.

Polyplex formation was further verified by gel electrophoresis. The electrostatic interactions between polymers and plasmid neutralize the DNA's negative charge and polyplex migration down the agarose gel is retarded.²² Polymer–plasmid complexation was carried out in PBS as previously described in Polyplex Preparation. Gels were composed of 0.7% agarose and contained ethidium bromide (EtBr). Polyplexes were run at 100 V for 1 h against a 1 kb ladder and a plasmid control. A second gel electrophoresis, in which polymer and plasmid were complexed in the presence of 4 mg/mL heparin, was also performed for comparison purposes. Heparin is a negatively charged polysaccharide used to mimic in vivo interactions between cationic polymers and negatively charged proteins/proteins.²³ Detailed protocols for both these assays can be found in the Supporting Information.

Polyplex Size and Zeta Potential. To determine polyplex size, polymer and pEGFP-N1 were complexed in 2 mL of deionized water at N/P ratios of 1, 5, 10, 20, and 40. Hydrodynamic size measurements of polymer–plasmid complexes were obtained by dynamic light scattering (DLS). The hydrodynamic radius measured by the DLS is calculated from the Stokes–Einstein equation, $D = kT / 6\pi\eta Rh$, where k is the Boltzmann constant, T is the temperature, η is the medium viscosity, and $f = 6\pi\eta Rh$ is the frictional coefficient for a hard sphere in a viscous medium.²⁴

For zeta potential measurements, polymer–plasmid solutions were prepared at N/P ratios of 1, 5, 10, 20, and 40 in 0.8 mL of deionized water. Zeta potential measurements were performed using a Malvern Zetasizer Nano ZS 90 particle analyzer.

Serum Stability. An agarose gel assay was used to determine polyplex stability under in vivo mimicking conditions. Briefly, polymer–plasmid complexes were incubated in PBS, pH 7.4, for 45 min at RT for complexation to occur. After the initial complexation time, heparin was added to the polyplex solution at a final volume of 4 mg/mL heparin and the polyplexes were incubated for another 30 min at RT. Complexes were then run on a 0.7% agarose gel containing EtBr against a 1 kb ladder and a plasmid control for 1 h at 100 V.

DNase I Protection Assay. For successful gene delivery, polymeric carriers must protect gene cargo from in vivo enzymatic degradation. A DNase I protection assay was performed to determine the DNA protection potential of thiolated polymers relative to the

unmodified polymer. Briefly, polymer–plasmid complexation was carried out in PBS as previously described. Polyplexes were subsequently added to a solution of 4 mg/mL heparin containing 0.1 unit/ μL DNase (human serum ranges between 2.0×10^{-4} and 8.2×10^{-2} unit/ μL enzyme activity) to mimic in vivo conditions.²⁵ After a 30 min incubation, complexes were run on an agarose gel as described above.

Buffering Capacity. A polymeric carrier's buffering capacity can affect its potential for endolysosomal escape and its delivery success.²⁶ Buffering capacity is defined as the percentage of positively charged groups that become protonated from pH 7.5–5.1.²⁷ It can be determined with an acid–base titration assay. Briefly, unmodified, 5, 13, and 20% thiol-modified polymers were added to 150 mM NaCl solution at a concentration of 0.2 mg/mL and the solutions were brought to a pH ~11 with NaOH. Then, 0.1 M HCl was added to polymer solutions in increments of 25 μL and the pH was measured at each point. The buffering capacity was calculated using the following equation:

$$\text{buffering capacity}(\%) = (\delta V_{\text{HCl}} \times 0.1\text{M}) / N(\text{mmol}) \times 100^{27}$$

where δV_{HCl} is the volume of the HCl solution (mL) needed to bring the pH from 7.4 to 5.1, 0.1 M is the concentration of the HCl, and N (mmol) is the total moles of polymer amines in each titration.

pH-Sensitive Gene Release. A DAPI assay was used to assess the polymer's potential to release the DNA cargo within the acidic environment of the cell. Briefly, polymer and plasmid were complexed at N/P ratios of 1, 5, 10, 20, and 40. Polyplex solutions were then brought to a pH of ~5.5 (late endosomal pH) using 0.1 M HCl and incubated for 30 min to allow for plasmid release. After the initial incubation period, DAPI was added to the solutions which were then incubated for an additional 30 min period. DAPI fluorescence was read at $\lambda_{\text{ex}} = 360$ nm and $\lambda_{\text{em}} = 455$ nm.

Statistical Analysis. All experiments were performed in triplicate. Data is presented as the average and corresponding standard deviation (error bar) of three ($n = 3$) separate sample trials. For zeta potential and DLS runs, multiple values were collected from each sample and outliers were identified by Grubbs's test and eliminated.

RESULTS AND DISCUSSION

Characterization of Thiolated Polymers. Using PAA as a model for a cationic polymer delivery vector, our goal was to improve the delivery potential of cationic polymers by generating pH-sensitive disulfide cross-linked modifications. By altering the concentration of 2-IT used in the synthesis reaction, we synthesized three thiolated polymers with 5, 13, or 20% thiol conjugation. The thiol percentage is a measure of how many primary amines on the PAA backbone were successfully conjugated with thiol-pendant chains. Thiolation was verified and quantified by a DNTB assay and by ^1H NMR.

According to the DNTB assay, 0.375, 0.75, and 1.5 mg/mL 2-IT synthesizes 5, 13, and 20% thiolated polymers, respectively (Table 1). ^1H NMR was performed on unmodified and 20% thiol-modified polymer in D_2O to verify thiolation. In the unmodified polymer, the methyl peak, adjacent to the primary amine, is located at 3.5 ppm. Thiol conjugation results in the formation of an additional peak at 2.6 ppm which signifies the

Table 1. Percent Thiolation Determined by Concentration of 2-IT

sample	PAA (mg/mL)	2-iminothiolane (mg/mL)	% of 1° amines thiolated
1	1	0	0
2	1	0.375	4.59 ± 2.43
3	1	0.75	13.07 ± 1.61
4	1	1.5	19.27 ± 0.074

presence of the methyl group adjacent to the thiol. An integration of the relative area under these two peaks verifies that the approximate 20% thiolation determined by the DNTB.

Validation of Disulfide Bonding. Other studies have shown that thiol conjugates can readily form cross-linked disulfide networks. PEGylated peptides can condense DNA through ionic interactions, as well as cross-linked networks formed by the spontaneous oxidation of cysteine thiols.⁵ Correlations between disulfide formation and solution viscosity indicate that thiol oxidation occurs more rapidly in viscous solutions. It is presumed that the close proximity of thiols in viscous solutions facilitates disulfide bonding.²⁰

Polyplex complexation was carried out at RT for 45 min and the extent of disulfide formation in all thiolated complexes was measured by a DNTB assay. Table 2 shows the percent of free

Table 2. Percentage of Thiols Present in Solutions after Polymer–Plasmid Complexation

N/P	5% thiol	13% thiol	20% thiol
1	97.19 ± 0.97	90.14 ± 3.90	91.32 ± 3.85
5	77.66 ± 0.76	90.39 ± 2.13	84.10 ± 6.95
10	52.26 ± 0.52	74.94 ± 3.43	55.37 ± 19.5
20	55.66 ± 0.48	66.54 ± 2.44	87.90 ± 6.46
40	69.41 ± 0.93	41.72 ± 3.32	84.44 ± 10.5

thiols present in solution after the 45 min incubation period. For 5 and 13% polymers, the general trend showed that the percentage of free thiols decreased, and therefore, the number of disulfides increased, with increasing N/P ratio. We believe that increased disulfide bonding in higher N/P complexes is due to the close proximity of thiols, as previously suggested by Maraschitz et al.²⁰ Overall, 5% thiolated polymers exhibited the highest degrees disulfide formation, followed by the 13% thiolated polymers. The exception was the N/P 40, 13% polyplexes which achieved the highest degree of cross-linking among all polymer samples. Interestingly, 20% thiolated polymers achieved very low disulfide binding. We believe that the additional amines from 2-IT increased the polymer's cationic charge, leading to greater repulsion among polymer chains and hindering disulfide formation.

DNA Binding Efficiency. Cationic polymers bind their genetic cargo through electrostatic interactions between the positively charged amines of the polymer and the negatively charged phosphates of the DNA backbone. The amines of a polymer backbone, however, have been linked to high cytotoxicity.^{28,29} Therefore, it would be beneficial to develop a carrier that can carry larger amounts of DNA cargo at lower polymer concentrations. To determine whether thiol cross-links can increase the amount of genetic cargo held by each carrier, the binding efficiencies of the unmodified and thiol-modified polymers were assessed using a DAPI displacement assay. DAPI is a fluorescent probe that interacts strongly with A-T base pairs of DNA. When bound to DNA, DAPI displays intense fluorescence at ex/em ~ 360/455 nm. The electrostatic interaction and complexation between polymer and DNA displaces DAPI and decreases fluorescence intensity. Hence, as DAPI fluorescence decreases, the polymer binding efficiency increases.²¹

The effect that thiolation and polymer concentration have on the fluorescence of DAPI-DNA is represented in Figure 2. Unmodified PAA had the least effect on fluorescence across all N/P ratios, suggesting weak PAA-DNA binding. This result was

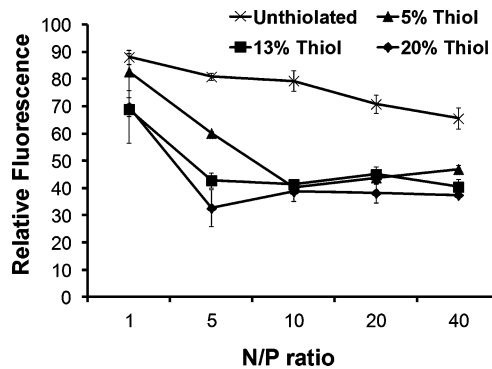


Figure 2. Displacement of DAPI from pEGFP-N1 by unmodified and thiolated polymers.

confirmed by gel electrophoresis on an agarose gel containing EtBr. Like DAPI, EtBr is an intercalating dye that only binds to free DNA or DNA that is not complexed with polymer. As a result, only free DNA is visible by gel electrophoresis.³⁰ The gel assay demonstrated that PAA cannot adequately bind DNA cargo (Figure 1 of the Supporting Information). PAA is a weak polyelectrolyte that has previously been shown to exhibit aggregation properties dependent on concentration, environmental pH, and aging times.³¹ In a study by Zhou et al.,³² discrete nanoparticles between PAA and DNA were formed at N/P values between 0.8 and 1.0, as determined by changes in light scattering. Further analysis by an EtBr displacement assay showed that at N/P ratios between 0.67 and 1.0 PAA decreased EtBr–DNA interactions, confirming some complexation. However, increasing the N/P ratio from 1.0 to 1.67 had no affect on EtBr–DNA binding. Zhou et al.³² concluded that, at higher PAA concentrations, EtBr–DNA interactions are independent of changes in the polymer concentration. In another study, Pathak et al.²² demonstrated that PAA–DNA complexation occurs only at very high polymer concentrations. This was done by running PAA–DNA complexes with polymer/plasmid weight ratios of 0.1, 0.2, and 0.3 $\mu\text{g}/\mu\text{g}$ on an agarose gel. According to the data, polyplex retardation occurred only at the highest polymer concentration, which is nearly 10-fold higher than that of our N/P 40 complexes.

Thiolation improves the polymer's ability to displace DAPI and bind with plasmid DNA. According to Figure 2, all thiolated polymers demonstrated greater efficiency in displacing DAPI than PAA across all N/P ratios. When 5, 13, and 20% thiolated polymer concentrations are increased from N/P 1 to 5, there is a sharp decrease in DAPI fluorescence. At N/P 10, DAPI fluorescence drops to values as low as ~40 au for all thiolated polymers. At N/P 20 and 40, DAPI fluorescence intensity is maintained between ~35–45 au. This suggests that past N/P 10 polymer-DNA binding is not greatly affected by the increasing polymer concentration.

Gel electrophoresis yielded similar results. While PAA complexes exhibited no retardation, migration of thiolated polyplexes was impeded at high N/P ratios. As seen in Figure 1 of the Supporting Information, thiolated polymers could not complex DNA at N/P 1, regardless of percent thiolation. Referring to the DAPI results (Figure 2), we see that, at N/P 1, even the highly thiolated 20% polymer decreases fluorescence by only 20 au with respect to the unmodified polymer. All thiolated polymers exhibited minimal cross-linking at N/P 1 (Table 2), which could potentially explain why complexation was unsuccessful. At higher N/P ratios, thiolated polyplexes

exhibited either partial or complete complexation. Partial complexation was evident by a faded plasmid strand, which suggests that only some of the DNA migrated through the gel. For some polyplexes, the DAPI assay and agarose gel showed conflicting results. For example, the 20% thiolated polymer displaced DAPI just as efficiently at N/P 5 as it did at N/P 40. However, at N/P 5, 20% thiolated polymers did not completely retard plasmid migration, whereas N/P 40 complexes did. We believe that the low DAPI fluorescence of 20% thiolated complexes can be attributed to the large size of the polymer. It is possible that the larger chain density of 20% thiolated polymers sterically hinders DAPI-plasmid interaction, thereby decreasing DAPI fluorescence. At the same time, the greater degree of disulfide cross-links in 5 and 13% thiolated complexes (Table 2) may have prevented plasmid migration along the gel.

Polymer–plasmid complexation was also performed in the presence of heparin to determine whether the negative charge of heparin would inhibit complexation. Resulting gel assays showed that in the presence of heparin, neither PAA nor thiolated polymers can complex DNA (see Figure 2 of the Supporting Information). The strong negative charge of heparin inhibited the electrostatic interaction of the polymer with the plasmid across all N/P ratios and thiol concentrations.

Complex Size and Stability. Formation of stable, nanosized polyplexes is an important prerequisite for successful cellular internalization. Optimal complex size varies between cell types, but spherical particles of ~100 nm are more amenable for internalization in cell culture and *in vivo*.³³ Polyplex stability, or the complex's ability to resist aggregation, also plays a vital role in successful gene delivery. Polyplex aggregation results in particles that are too large for efficient cellular uptake. In addition, polymer aggregates that accumulate at the cell surface can damage the plasma membrane. *In vivo*, polyplex aggregation prevents cargo from reaching target cells, and results in increased toxicity levels at the site of accumulation.^{4,29,34}

Polyplex size and stability were determined using dynamic light scattering (DLS) and zeta potential, respectively. The magnitude of the zeta potential indicates the stability of a colloidal system. Large negative or positive zeta potentials indicate that the particles repel each other. Repulsion limits particle aggregation and allows for a stable suspension to form. Generally, zeta potentials greater than +30 mV or lower than -30 mV indicate good stability. As the zeta potential approaches zero, particles in suspension tend to aggregate.³⁵

DLS data (Table 3) showed no consistent pattern for 5%, 13%, and unmodified polymer complexes. The size of unmodified PAA and 5% thiolated PAA polyplexes could not be determined at N/P 1 and N/P 5 due to large fluctuations in complex size. Based on the low zeta potentials corresponding to unmodified and 5% thiolated polymers at N/P 5, we believe the large polydispersity of these complexes results from complex instability. However, at N/P 1 both unmodified and 5% thiolated polymers have zeta potentials that are quite negative and thereby do not support the DLS data. The smallest complexes were formed by N/P 10–40, 5% polyplexes, which can be explained by the high degree of cross-linking in these polyplexes. The 13 and 20% thiolated polymers show more consistency between DLS and zeta potential measurements than the unmodified and 5% thiolated polymers. At N/P ratios of 1, 20, and 40, 13% thiolated polymers formed polyplexes of ~100 nm with a small standard deviation. N/P 5, 13% polyplexes, on the other hand exhibited a large size range which

Table 3. Polyplex Size and Zeta Potentials

% thiol	N/P	size (nm)	ζ (mV)
0	1		-20.00 ± 2.07
0	5		-6.75 ± 3.24
0	10	122.50 ± 33.45	4.74 ± 4.47
0	20	100.85 ± 21.88	10.75 ± 3.07
0	40	105.48 ± 7.55	16.00 ± 0.53
5	1		-27.53 ± 1.16
5	5		-15.68 ± 5.63
5	10	63.05 ± 23.22	11.36 ± 3.79
5	20	71.45 ± 20.09	17.83 ± 1.63
5	40	91.63 ± 14.03	19.73 ± 0.21
13	1	104.05 ± 5.72	-34.00 ± 1.87
13	5	91.94 ± 48.51	4.26 ± 0.52
13	10	191.85 ± 24.17	35.90 ± 1.25
13	20	100.56 ± 8.98	38.23 ± 0.75
13	40	105.05 ± 4.80	41.77 ± 2.67
20	1	80.76 ± 10.01	-35.37 ± 1.07
20	5	87.72 ± 7.95	24.13 ± 2.76
20	10	99.72 ± 5.02	31.87 ± 2.82
20	20	117.61 ± 5.25	38.87 ± 5.79
20	40	124.09 ± 2.74	41.40 ± 1.57

can be explained by the low zeta potential of these complexes. The exception to this set of polyplexes were the N/P 10 complexes which were nearly twice as large in size. Finally, the 20% thiolated polymers showed the greatest consistency between DLS and zeta potential data. Complexes obtained from the 20% thiol-modified polymer reached absolute zeta potential values between 25 and 40 mV, and ranged between 80 and 125 nm. Because 20% thiolated polymers did not demonstrate high degrees of thiol cross-linking, we believe that polyplex formation resulted primarily from electrostatic interactions between polymer strands and plasmid cargo.

Heparin-Induced Decomplexation. Typically, *in vitro* polymeric gene delivery assays are carried out in serum-free medium to avoid the polymer–protein interactions that inhibit polyplex internalization. *In vivo*, however, cationic polymer–protein interactions cannot be avoided. Negatively charged serum proteins aggregate around polymer–plasmid complexes. As a result, polyplexes are destabilized, and the DNA is left susceptible to enzymatic degradation. Hence, we evaluated the polymers potential to maintain complex stability in a more physiologically relevant system, for example, in the presence of heparin, a negatively charged polysaccharide used to mimic potential polyplex interactions with serum proteins.²³

Thiolated polymers were complexed in PBS, then exposed to heparin for 30 min, and finally run on an agarose gel to evaluate the degree of decomplexation. Figure 3 shows that thiolated polymers decomplexed at low N/P ratios but remained intact at higher N/P ratios. The 5 and 20% thiolated polymers maintained polyplex stability at N/P ratios of 10, 20, and 40, decomplexing only at N/P 1 and 5. The 13% thiolated polyplexes decomplexed only at N/P 1. Unmodified PAA showed complete decomplexation. However, from the complexation assay (Figure 1 of the Supporting Information), we know that PAA never complexed with plasmid. Further, when comparing the complexation and decomplexation assays, it becomes evident that polyplexes that were only partially complexed in the complexation assay (Figure 1 of the Supporting Information) completely decomplexed in the presence of heparin (Figure 3). From the data, it appears

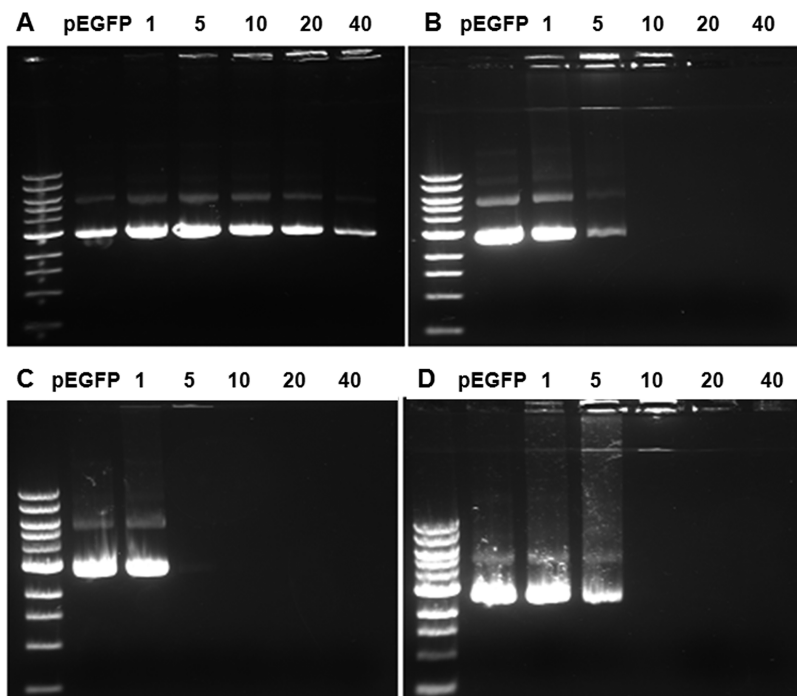


Figure 3. Agarose gel of unmodified PAA (A), 5% (B), 13% (C), and 20% (D) thiolated polyplexes after suspension in a heparin solution.

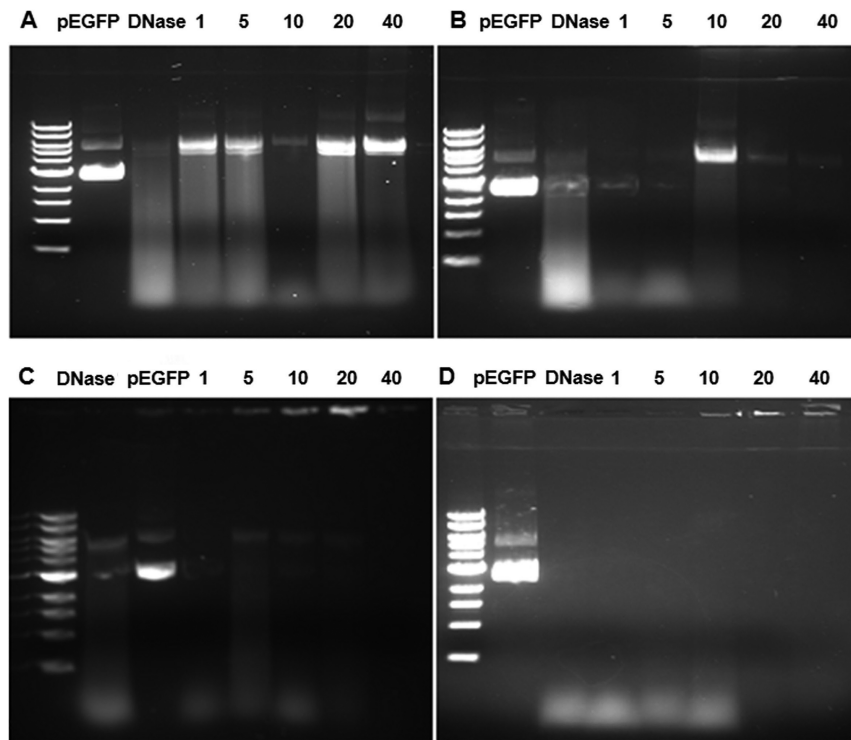


Figure 4. Agarose gel of unmodified PAA (A), 5% (B), 13% (C), and 20% (D) thiolated polyplexes after exposure to DNase I in a heparin solution.

that overall the 13% thiolated polymer would be a better carrier choice for improved gene binding and release.

DNase I Protection Assay. For a polymeric delivery vector to be clinically successful, it must not only bind DNA, but must also protect the cargo from degradative enzymes present in the host circulatory system. Results obtained from the heparin-induced decomplexation assay suggested that at higher N/P ratios thiolated polymers have the ability to maintain polyplex

structure in the presence of serum proteins. These polymers should therefore also be more efficient at protecting gene cargo than unmodified polymer carriers. To determine whether thiol cross-links improve gene protection, a DNase I protection assay was performed. In vivo, human serum contains between 2.0×10^{-4} and 8.2×10^{-2} unit/ μL enzyme activity. To mimic these conditions, polyplexes were complexed in plasmid, then added to a heparin solution, and finally treated with 0.1 unit/ μL

DNase I.²⁵ Samples were subsequently run on a 0.7% agarose gel to determine DNA degradation.

Results showed that weakly bound PAA (Figure 4) could not protect plasmid from DNase degradation across all N/P ratios. Thiolated polymers, on the other hand, successfully protected the plasmid at N/P ratios of 20 and 40, but left the plasmid susceptible to degradation at lower N/P ratios. The 20% thiolated polyplexes completely degraded at N/P 1, 5, and 10, which could potentially be explained by the poor disulfide-linking of these polyplexes. The 5 and 13% thiolated polymers performed better than the 20% complexes, exhibiting only partial plasmid degradation. Partial degradation is evident by the presence of two bands, a degraded DNA band and an intact DNA band. The 13% thiolated polymers showed some enzymatic degradation at N/P 1–20, but completely protected the DNA with the highly cross-linked N/P 40 polyplexes. The 5% thiolated polyplexes exhibited partial degradation across all N/P ratios. It is possible that the greater enzymatic protection in 5 and 13% polyplexes resulted from the higher degree of disulfide cross-linking.

When comparing the data acquired from the “Heparin-Induced Decomplexation” assay and the “DNase I Protection Assay”, it becomes evident that some samples which resisted decomplexation in the presence of heparin, did not completely protect the DNA cargo in the DNase I assay. For example, 13% thiolated polyplexes with N/P > 5 remained intact in the presence of heparin (Figure 3c). Based on this data, it could be inferred that these complexes would completely resist DNase I degradation. However, Figure 4c shows partial DNA degradation in these samples. We believe that heparin–polymer interactions were not strong enough to completely decomplex polyplexes and release plasmid cargo, but that the presence of heparin was sufficient to destabilize complexes, leaving some of the DNA susceptible to degradation.

Buffering Capacity and Endosomal Escape. Due to size restrictions, polyplexes typically cannot diffuse into cells and must be taken up by endocytosis, a multistep process in which cells internalize molecules from the extracellular space by engulfing them within the cell membrane. A portion of the membrane invaginates and pinches off from the cell forming a membrane bound vesicle known as the endosome. Upon internalization, the endosome has a pH ~ 7, which ultimately drops to pH ~ 4 as the vesicle matures from an endosome to a lysosome.³⁶ Polyplexes that do not escape the endolysosome are eventually degraded. Although more than 95% of cells in a culture internalize polyplexes during a given transfection, less than 50% of cells express the gene.² From this standpoint, a polymer's success is dependent on its ability to buffer the endolysosomal pH, which has been shown to facilitate polyplex escape into the cell cytosol via the proton-sponge effect.^{2,37} To determine whether thiol groups can improve the buffering capacity of cationic polymers, we performed a titration assay in which 0.1 M HCl was added to polymer solutions in increments of 25 μL and the change in pH was recorded. Polymers with a high buffering capacity contain larger amounts of protonizable groups. As a result of this buffering effect, a greater amount of protons, or acid must be added to the solution for the pH to drop. Because disulfides are readily reduced in the presence of protons, increasing the number of thiols conjugated onto the polymer backbone improves the polymers buffering capacity. Each polymer's buffering capacity was calculated as the percentage of amine groups being protonated when the pH drops from pH 7.0 to 5.1, conditions

mimicking the change from the extracellular environment to the low pH of the endosome.²⁷ The results showed that the presence of thiols can drastically improve the polymers buffering capacity. The 20% thiolated polymers had a buffering capacity of ~47%, which was more than double the buffering capacity of unmodified polymer (~19%). The 5% and 13% polymers attained buffering capacities of ~30 and ~36, respectively. The improvement in buffering capacity is evident in the titration curves obtained (Figure 5).

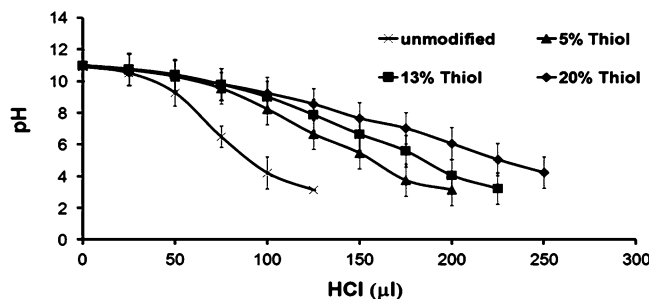


Figure 5. pH titration of unmodified PAA (A), 5% (B), 13% (C), and 20% (D) thiolated polymers to determine buffering capacity.

pH-Sensitive Gene Release. Polymeric carriers that depend solely on strong electrostatic interactions to bind gene cargo often experience inefficient cargo release; the polymer remains bound to the DNA even within the cell. As a result, the delivered DNA never reaches the nucleus where gene expression takes place. The binding efficiency studies showed that, at higher N/P ratios, thiolated polymers were able to successfully complex DNA. A pH-sensitive gene release assay was performed to determine whether a thiolated polymer could release its cargo within the endosome before reaching lysosomal degradation. Figure 6 shows the relative fluorescence of DAPI-labeled DNA of unmodified and thiolated polyplexes at N/P ratios of 1, 5, 10, 20, and 40. At endosomal pH 5.5, unmodified and 5% thiolated polymers showed very low (if any) gene release. The high fluorescence intensities observed in the unmodified polyplex solutions once again verified that PAA does not adequately bind DNA. The 5% thiolated polyplexes, on the other hand, exhibited low fluorescence intensities at pH 7.0, suggesting high binding efficiency. The previous DAPI displacement and gel assays demonstrated that the 5% thiolated polymer was the most efficient at binding DNA. This data verified that result and also showed that 5% polyplexes did not adequately release DNA; polymer–plasmid complexes remained bound even at the low pH of 5.5. The 20% thiol polyplexes exhibited high cargo binding and release only at N/P ratios of 20 and 40. At N/P 1, 5, and 10, 20% thiolated polymers did not appear to sufficiently bind cargo DNA. This result can also be seen in the gel assay (Figure 1 of the Supporting Information). Finally, the 13% polymer appeared to have the highest binding-release capabilities out of all thiolated polymers, with the N/P 40 ratio being the exception. As demonstrated by the DNTB assay, 13%, N/P 5 polyplexes displayed the greatest amount of cross-linking among all polymer samples. Based on this data it can be inferred that an optimal combination of charge ratio and thiol cross-links are required for high binding and release kinetics.

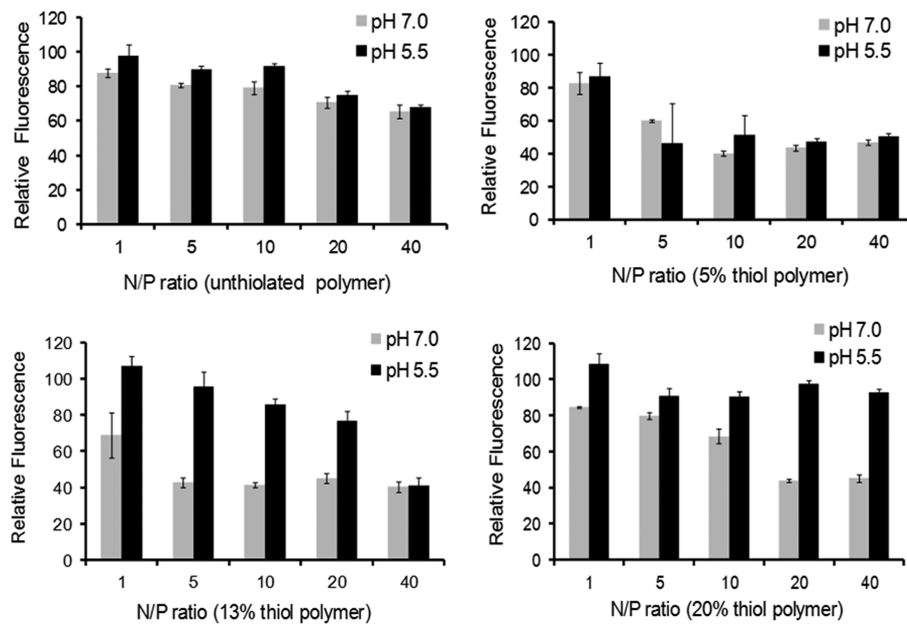


Figure 6. pH-sensitive plasmid release determined by a DAPI displacement assay.

CONCLUSIONS

A successful polymeric carrier for nonviral gene delivery must overcome a number of challenging extracellular and intracellular obstacles. Our data demonstrates that a certain degree of thiolation can significantly improve the carrier's *in vivo* potential. From our data, we can conclude that the 5% thiolated complexes would be inefficient polymeric carriers because of their low gene release. Although these complexes bind and protect DNA more efficiently than 13 and 20% thiolated polymers, they exhibit minimal (if any) gene release at endosomal pH. The 5% thiolated polyplexes also demonstrated the greatest amount of cross-linking overall. We therefore believe that too many cross-links hinder the polymer's delivery potential. At the same time, the 20% thiolated polymer, which had the greatest buffering capacity and potential for endolysosomal escape, was also inefficient at DNA binding and release. Further, 20% thiolated polymers were the least effective in protecting gene cargo. The N/P 20 and 40, 20% thiolated polyplexes were the exception to the 20% polyplex formulations, exhibiting high binding and release kinetics. Therefore, the polyplexes with the greatest delivery potential overall were the 13% thiolated polymers. Although 13% polyplexes showed partial degradation in the presence of DNase, they also achieved approximately twice the buffering capacity of PAA and were typically better at binding and releasing DNA.

Altogether, our results show that a certain degree of thiolation can markedly improve the polymeric carrier's performance under conditions that mimic both the extracellular and the intracellular environment, therefore, holding promise to improve *in vivo* delivery. This paper has addressed the major extracellular barriers of gene delivery, including polymer–gene binding efficiency, polyplex size, and stability in the presence of degradative enzymes and other proteins. In the future, *in vitro* transfection and cytotoxicity assays will be performed using pEGFP-N1 plasmid to determine how thiolation affects the polymer's delivery success.

ASSOCIATED CONTENT

S Supporting Information

Experimental details and additional figures. This material is available free of charge via the Internet at <http://pubs.acs.org>.

AUTHOR INFORMATION

Corresponding Author

*E-mail: kofinas@umd.edu.

Notes

The authors declare no competing financial interest.

REFERENCES

- (1) Gabrielson, N. P.; Pack, D. W. *Biomacromolecules* **2006**, *7* (8), 2427–2435.
- (2) Pack, D. W.; Hoffman, A. S.; Pun, S.; Stayton, P. S. *Nat. Rev. Drug Discovery* **2005**, *4* (7), 581–593.
- (3) Putnam, D. *Nat. Mater.* **2006**, *5* (6), 439–51.
- (4) Morille, M.; Passirani, C.; Vonarbourg, A.; Clavreul, A.; Benoit, J. P. *Biomaterials* **2008**, *29* (24–25), 3477–3496.
- (5) Kim, S. W.; Kim, T. I. *React. Funct. Polym.* **2011**, *71* (3), 344–349.
- (6) Mintzer, M. A.; Simanek, E. E. *Chem. Rev.* **2009**, *109* (2), 259–302.
- (7) Mastrobattista, E.; Hennink, W. E. *Nat. Mater.* **2012**, *11* (1), 10–12.
- (8) Kim, S. W.; Kim, T.; Rothmund, T.; Kissel, T. *J. Controlled Release* **2011**, *152* (1), 110–119.
- (9) Cho, C. S.; Jere, D.; Arote, R.; Jiang, H. L.; Kim, Y. K.; Cho, M. H. *Biomed. Mater.* **2009**, *4*, 2.
- (10) Zhao, Q. Q.; Chen, J. L.; Lv, T. F.; He, C. X.; Tang, G. P.; Liang, W. Q.; Tabata, Y.; Gao, J. Q. *Biol. Pharm. Bull.* **2009**, *32* (4), 706–710.
- (11) Safinya, C. R.; Koltover, I.; Wagner, K. *Proc. Natl. Acad. Sci. U.S.A.* **2000**, *97* (26), 14046–14051.
- (12) Synatschke, C. V.; Schallau, A.; Jerome, V.; Freitag, R.; Muller, A. H. *Biomacromolecules* **2011**, *12* (12), 4247–4255.
- (13) Xiong, M. P.; Forrest, M. L.; Ton, G.; Zhao, A.; Davies, N. M.; Kwon, G. S. *Biomaterials* **2007**, *28* (32), 4889–4900.
- (14) Godbey, W. T.; Wu, K. K.; Mikos, A. G. *J. Biomed. Mater. Res.* **1999**, *45* (3), 268–275.
- (15) Georgiou, T. K.; Vamvakaki, M.; Patrickios, C. S.; Yamasaki, E. N.; Phylactou, L. A. *Biomacromolecules* **2004**, *5* (6), 2221–2229.

- (16) vandeWetering, P.; Cherng, J. Y.; Talsma, H.; Hennink, W. E. *J. Controlled Release* **1997**, *49* (1), 59–69.
- (17) Pafiti, K. S.; Mastroyiannopoulos, N. P.; Phylactou, L. A.; Patrickios, C. S. *Biomacromolecules* **2011**, *12* (5), 1468–1479.
- (18) Peng, Q.; Hu, C.; Cheng, J.; Zhong, Z.; Zhuo, R. *Bioconjugate Chem.* **2009**, *20* (2), 340–6.
- (19) Mok, H.; Park, T. G. *Macromol. Biosci.* **2009**, *9* (8), 731–743.
- (20) Marschutz, M. K.; Bernkop-Schnurch, A. *Eur. J. Pharm. Sci.* **2002**, *15* (4), 387–394.
- (21) Deshpande, M. C.; Garnett, M. C.; Vamvakaki, M.; Bailey, L.; Armes, S. P.; Stolnik, S. *J. Controlled Release* **2002**, *81* (1–2), 185–199.
- (22) Pathak, A.; Aggarwal, A.; Kurupati, R. K.; Patnaik, S.; Swami, A.; Singh, Y.; Kumar, P.; Vyas, S. P.; Gupta, K. C. *Pharm. Res.* **2007**, *24* (8), 1427–1440.
- (23) Xu, P. S.; Quick, G. K.; Yeo, Y. *Biomaterials* **2009**, *30* (29), 5834–5843.
- (24) Giacomelli, C.; Lafitte, G.; Borsali, R. *Macromol. Symp.* **2005**, *229*, 107–117.
- (25) Arima, H.; Kihara, F.; Hirayama, F.; Uekama, K. *Bioconjugate Chem.* **2001**, *12* (4), 476–484.
- (26) Tseng, S. J.; Tang, S. C.; Shau, M. D.; Zeng, Y. F.; Cherng, J. Y.; Shih, M. F. *Bioconjugate Chem.* **2005**, *16* (6), 1375–1381.
- (27) Ou, M.; Wang, X. L.; Xu, R.; Chang, C. W.; Bull, D. A.; Kim, S. W. *Bioconjugate Chem.* **2008**, *19* (3), 626–33.
- (28) Cho, C. S.; Yu, J. H.; Huang, J.; Jiang, H. L.; Quan, J. S.; Cho, M. H. *J. Appl. Polym. Sci.* **2009**, *112* (2), 926–933.
- (29) Fischer, D.; Li, Y. X.; Ahlemeyer, B.; Kriegstein, J.; Kissel, T. *Biomaterials* **2003**, *24* (7), 1121–1131.
- (30) Ikonen, M.; Murtomaki, L.; Kontturi, K. *Colloids Surf., B* **2008**, *66* (1), 77–83.
- (31) Park, J.; Choi, Y. W.; Kim, K.; Chung, H.; Sohn, D. *Bull. Korean Chem. Soc.* **2008**, *29* (1), 104–110.
- (32) Zhou, Y. L.; Li, Y. Z. *Biophys. Chem.* **2004**, *107* (3), 273–281.
- (33) Merdan, T.; Kopecek, J.; Kissel, T. *Adv. Drug Delivery Rev.* **2002**, *54* (5), 715–58.
- (34) Fishbein, I.; Chorny, M.; Levy, R. J. *Curr. Opin. Drug Discovery Dev.* **2010**, *13* (2), 203–213.
- (35) Mandzy, N.; Grulke, E.; Druffel, T. *Powder Technol.* **2005**, *160* (2), 121–126.
- (36) Varga, C. M.; Wickham, T. J.; Lauffenburger, D. A. *Biotechnol. Bioeng.* **2000**, *70* (6), 593–605.
- (37) Thomas, M.; Klibanov, A. M. *Appl. Microbiol. Biotechnol.* **2003**, *62* (1), 27–34.